

# Selective Ring-Opening of Di-Substituted Epoxides Catalysed by Halohydrin Dehalogenases

Elia Calderini,<sup>[a]</sup> Julia Wessel,<sup>[a]</sup> Philipp Süß,<sup>[b]</sup> Patrick Schrepfer,<sup>[a]</sup> Rainer Wardenga,<sup>[b]</sup> and Anett Schallmeyer<sup>\*[a]</sup>

Halohydrin dehalogenases (HHDHs) are valuable biocatalysts for the synthesis of  $\beta$ -substituted alcohols based on their epoxide ring-opening activity with a number of small anionic nucleophiles. In an attempt to further broaden the scope of substrates accepted by these enzymes, a panel of 22 HHDHs was investigated in the conversion of aliphatic and aromatic vicinally di-substituted *trans*-epoxides using azide as nucleophile.

The majority of these HHDHs was able to convert aliphatic methyl-substituted epoxide substrates to the corresponding azidoalcohols, in some cases even with absolute regioselectivity. HheG from *Ilumatobacter coccineus* exhibited also high activity towards sterically more demanding di-substituted epoxides. This further expands the range of  $\beta$ -substituted alcohols that are accessible by HHDH catalysis.

## Introduction

Enzymes are attractive catalysts as they offer the possibility to attain building blocks through highly regio-, stereo-, and chemoselective transformations. In this sense, halohydrin dehalogenases (HHDHs, also called haloalcohol dehalogenases or halohydrin hydrogen-halide-lyases), initially discovered for their ability to degrade halogenated compounds,<sup>[1]</sup> are very useful biocatalysts that catalyse the reversible dehalogenation of vicinal haloalcohols via formation of the corresponding epoxides.<sup>[2,3]</sup> For a practical application of HHDHs, their promiscuous epoxide ring-opening activity with a range of small anionic nucleophiles such as azide, cyanide, nitrite, cyanate or thiocyanate is even more attractive as it enables the regio- and stereoselective formation of novel C–N, C–C, C–O and C–S bonds.<sup>[4,5]</sup> Hence, HHDH-catalysed reactions give access to synthetically important  $\beta$ -substituted alcohols and chiral epoxides. Biocatalytic examples include the synthesis of ethyl (*R*)-4-cyano-3-hydroxybutyrate, a chiral synthon for the production of statin side chains,<sup>[6]</sup> enantiopure epihalohydrins,<sup>[7,8]</sup> highly enantioenriched oxazolidinones<sup>[9]</sup> and tertiary alcohols.<sup>[10,11]</sup>

HHDHs belong to the superfamily of short-chain dehydrogenases/reductases (SDR). In contrast to other SDR enzymes, their catalytic mechanism does not require any cofactor.<sup>[12]</sup> In HHDHs, the cofactor binding pocket found in SDR enzymes is

replaced by a nucleophile binding pocket.<sup>[13]</sup> Moreover, they feature a conserved catalytic triad composed of Ser–Tyr–Arg, which acts in a concerted manner to catalyse the epoxide formation and concomitant halide release.<sup>[13,14]</sup> In the epoxide ring-opening reaction, the nucleophilic attack typically occurs at the sterically less-hindered carbon atom following an  $S_N2$  mechanism.<sup>[15]</sup> Until recently, only terminal epoxides had been reported to be accepted as substrates by HHDHs. When studying HheC from *Agrobacterium tumefaciens*, HheA2 from *Arthrobacter* sp. AD2 and HheB2 from *Mycobacterium* sp. GP1 for their activity on vicinally di-substituted as well as cyclic epoxides, Majeric Elenkov et al. found that none of the tested HHDHs exhibited activity towards these sterically more demanding epoxides.<sup>[16]</sup> Only in one paper by Hasnaoui-Dijoux et al., it is briefly noted that HheC was observed to catalyse the ring-opening of 2,3-epoxyheptane with nitrite as nucleophile but without experimental detail.<sup>[4]</sup>

We recently reported the identification of a large set of novel HHDH enzymes based on a database mining approach using HHDH-specific sequence motifs.<sup>[17]</sup> Together with the five previously known HHDHs, they compose a broad family of HHDH enzymes subdivided into six phylogenetic subtypes A through G. A representative subset of 17 novel HHDHs, which span the entire phylogenetic tree, was subsequently cloned and biocatalytically characterised.<sup>[18]</sup> This way, HheG from *Ilumatobacter coccineus* was found to convert cyclic epoxides such as cyclohexene oxide and limonene oxide with synthetic useful activity.<sup>[19]</sup> This represents the first example for the ring-opening of cyclic epoxide substrates using a halohydrin dehalogenase.

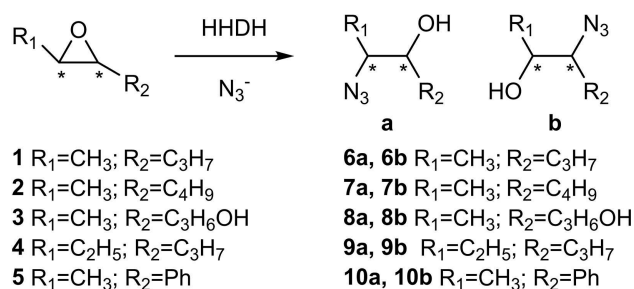
Intrigued by this finding, we aimed to study also other vicinally di-substituted but non-cyclic epoxides as substrates in bioconversions with halohydrin dehalogenases. Employing a representative set of 19 new and three previously known HHDH enzymes, we screened for activity towards five different racemic di-substituted *trans*-epoxides with aliphatic or aromatic substituents using azide as nucleophile (Scheme 1). The resulting azidoalcohols are useful intermediates for the synthesis of corresponding aliphatic and arylaliphatic aminoalcohols. This is

[a] E. Calderini, Dr. J. Wessel, Dr. P. Schrepfer, Prof. Dr. A. Schallmeyer  
Institute for Biochemistry, Biotechnology and Bioinformatics  
Technische Universität Braunschweig  
Spielmannstr. 7, 38106 Braunschweig (Germany)  
E-mail: a.schallmeyer@tu-braunschweig.de

[b] Dr. P. Süß, Dr. R. Wardenga  
Enzymicals AG  
Walther-Rathenau-Straße 49A, 17489 Greifswald (Germany)

Supporting information for this article is available on the WWW under <https://doi.org/10.1002/cctc.201900103>

© 2019 The Authors. Published by Wiley-VCH Verlag GmbH & Co. KGaA.  
This is an open access article under the terms of the Creative Commons Attribution Non-Commercial NoDerivs License, which permits use and distribution in any medium, provided the original work is properly cited, the use is non-commercial and no modifications or adaptations are made.



**Scheme 1.** HHDH-catalysed azidolysis of racemic di-substituted *trans*-epoxides (1–5) resulting in the formation of two possible regioisomeric azidoalcohols (6–10).

the first comprehensive study of the ring-opening of vicinally di-substituted epoxides catalysed by a large set of HHDHs.

## Results and Discussion

A subset of 22 HHDHs from our panel, containing enzymes from all six phylogenetic HHDH subtypes, was tested in bioconversions of racemic di-substituted *trans*-epoxides 1–5 using azide as exemplary nucleophile (Scheme 1). As a result, 17 (including HheC) out of 22 tested HHDHs displayed activity in the conversion of the two aliphatic substrates *trans*-2,3-epoxyhexane (1) and *trans*-2,3-epoxyheptane (2), affording the corresponding azidoalcohols in varying yields (Table 1). In contrast, significantly less HHDHs converted the sterically more demanding epoxides *trans*-4,5-epoxyhexan-1-ol (3), *trans*-3,4-epoxyheptane (4) and *trans*- $\beta$ -methylstyrene oxide (5). HheG

from *Ilumatobacter coccineus* was active on all five epoxide substrates yielding highest conversion for substrates 1, 3, 4 and 5 among all tested HHDHs. Significant conversion of 5 by HheG was unexpected as the enzyme was shown to exhibit only very little activity on styrene oxide.<sup>[18]</sup> For HheA2 and HheB2, hardly any product formation in the conversion of the tested vicinally di-substituted epoxides was observed, which is in agreement with previous findings.<sup>[15]</sup>

Interestingly, addition of a terminal hydroxyl group, as present in substrate 3, abolished activity of all tested HHDHs that displayed activity on the corresponding non-hydroxylated epoxide 1, except for HheG. Though this hydroxyl group is at the opposite end of the aliphatic molecule compared to the epoxide ring, it can support unproductive binding of the substrate in the enzyme active site (see also below). Surprisingly, only HheG, but not HheG2, is able to convert epoxide 3, albeit both enzymes share 74% sequence identity on protein level.<sup>[19]</sup>

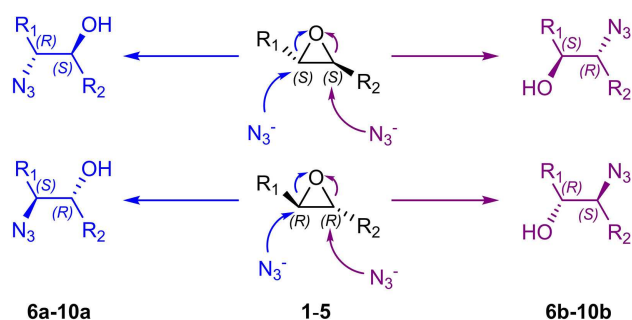
Comparing substrates 2 and 4, which differ in the position of their epoxide ring, only a reduced number of HHDHs was still active on *trans*-3,4-epoxyheptane (4). Enzymes HheA3, HheD, HheD2, HheD3 and HheD5, as well as HheG2 gave low to moderate conversions, whereas HheG converted 4 completely within 15 h reaction time.

The vicinally di-substituted epoxide substrates 1–5 each contain two stereocentres. Depending on the site of nucleophilic attack and the stereoconfiguration of the substrate during HHDH-catalysed epoxide ring-opening, two regioisomers and their respective pairs of enantiomers can be attained (Scheme 2). Thus, the regioselectivity of active HHDHs in the conversion of substrates 1–5 was studied. Most enzymes formed both regioisomeric products **a** and **b** in varying ratios

**Table 1.** Substrate conversions and ratio of formed regioisomeric products **a:b** obtained in biocatalytic reactions of substrates 1–5 with HHDHs using azide as nucleophile. All biotransformations were performed in duplicate.

HDDH <sup>[a]</sup>	Conversion [%] (ratio of regioisomeric products <b>a:b</b> )				
	1	2	3	4	5
HheA2	3.1 ± 0.2 (n.d. <sup>[b]</sup> )	3.1 ± 0.2 (76:24)	< 0.01 (n.d. <sup>[b]</sup> )	< 0.01 (n.d. <sup>[b]</sup> )	0.8 ± < 0.1 (n.d. <sup>[b]</sup> )
HheA3	52 ± < 0.1 (92:8)	97 ± < 0.1 (97:3)	< 0.01 (n.d. <sup>[b]</sup> )	1.2 ± 0.3 (n.d. <sup>[b]</sup> )	0.9 ± 0.1 (n.d. <sup>[b]</sup> )
HheA5	3.6 ± < 0.1 (n.d. <sup>[b]</sup> )	6.1 ± < 0.1 (98:2)	< 0.01 (n.d. <sup>[b]</sup> )	< 0.01 (n.d. <sup>[b]</sup> )	0.5 ± < 0.1 (n.d. <sup>[b]</sup> )
HheB2	5.4 ± < 0.1 (n.d. <sup>[b]</sup> )	5.6 ± < 0.1 (88:12)	n.d. <sup>[b]</sup>	n.d. <sup>[b]</sup>	n.d. <sup>[b]</sup>
HheB3	13 ± 0.9 (73:27)	13 ± 0.7 (67:33)	< 0.01 (n.d. <sup>[b]</sup> )	< 0.01 (n.d. <sup>[b]</sup> )	0.6 ± < 0.1 (n.d. <sup>[b]</sup> )
HheB4	< 0.1 (n.d. <sup>[b]</sup> )	0.2 ± < 0.1 (n.d. <sup>[b]</sup> )	< 0.01 (n.d. <sup>[b]</sup> )	< 0.01 (n.d. <sup>[b]</sup> )	0.5 ± 0.1 (n.d. <sup>[b]</sup> )
HheB5	59 ± 1.6 (88:12)	97 ± 0.1 (87:13)	< 0.01 (n.d. <sup>[b]</sup> )	< 0.01 (n.d. <sup>[b]</sup> )	0.5 ± 0.1 (n.d. <sup>[b]</sup> )
HheB6	76 ± 5.3 (90:10)	100 ± 0.1 (89:11)	< 0.01 (n.d. <sup>[b]</sup> )	< 0.01 (n.d. <sup>[b]</sup> )	0.5 ± < 0.1 (n.d. <sup>[b]</sup> )
HheB7	81 ± 2.4 (90:10)	100 ± < 0.1 (89:11)	< 0.01 (n.d. <sup>[b]</sup> )	< 0.01 (n.d. <sup>[b]</sup> )	0.6 ± < 0.1 (n.d. <sup>[b]</sup> )
HheC	44 ± 12.6 (97:3)	100 ± 0.4 (98:2)	< 0.01 (n.d. <sup>[b]</sup> )	< 0.01 (n.d. <sup>[b]</sup> )	0.6 ± 0.3 (n.d. <sup>[b]</sup> )
HheD	44 ± 2.8 (50:50)	94 ± 1.3 (55:45)	< 0.01 (n.d. <sup>[b]</sup> )	8.6 ± 0.2 (55:45)	0.5 ± 0.2 (n.d. <sup>[b]</sup> )
HheD2	64 ± 2.2 (50:50)	90 ± 4.9 (50:50)	< 0.01 (n.d. <sup>[b]</sup> )	2.6 ± 0.1 (69:31)	0.6 ± < 0.1 (n.d. <sup>[b]</sup> )
HheD3	88 ± 3.8 (50:50)	100 ± < 0.1 (57:43)	< 0.01 (n.d. <sup>[b]</sup> )	25 ± 2.2 (69:31)	1.1 ± 0.3 (7:93)
HheD5	100 ± < 0.1 (64:36)	100 ± < 0.1 (50:50)	< 0.01 (n.d. <sup>[b]</sup> )	4.5 ± 0.6 (49:51)	0.7 ± < 0.1 (n.d. <sup>[b]</sup> )
HheE	100 ± < 0.1 (98:2)	100 ± < 0.1 (99:1)	< 0.01 (n.d. <sup>[b]</sup> )	< 0.01 (n.d. <sup>[b]</sup> )	0.4 ± 0.2 (n.d. <sup>[b]</sup> )
HheE2	12 ± < 0.1 (91:9)	85 ± < 0.1 (98:2)	< 0.01 (n.d. <sup>[b]</sup> )	< 0.01 (n.d. <sup>[b]</sup> )	0.7 ± 0.1 (n.d. <sup>[b]</sup> )
HheE3	16 ± < 0.1 (89:11)	92 ± < 0.1 (99:1)	< 0.01 (n.d. <sup>[b]</sup> )	< 0.01 (n.d. <sup>[b]</sup> )	0.5 ± 0.1 (n.d. <sup>[b]</sup> )
HheE4	< 0.1 (n.d. <sup>[b]</sup> )	15 ± < 0.1 (97:3)	< 0.01 (n.d. <sup>[b]</sup> )	< 0.01 (n.d. <sup>[b]</sup> )	0.6 ± < 0.1 (n.d. <sup>[b]</sup> )
HheE5	86 ± < 0.1 (98:2)	100 ± < 0.1 (99:1)	< 0.01 (n.d. <sup>[b]</sup> )	< 0.01 (n.d. <sup>[b]</sup> )	0.7 ± < 0.1 (n.d. <sup>[b]</sup> )
HheF	56 ± 0.7 (86:14)	70 ± 2.1 (83:17)	< 0.01 (n.d. <sup>[b]</sup> )	< 0.01 (n.d. <sup>[b]</sup> )	1.3 ± 0.2 (13:87)
HheG	100 ± < 0.1 (50:50)	100 ± 0.1 (60:40)	49 ± 9.3 (92:8)	99 ± 0.1 (51:49)	44 ± 1.9 (0.4:99.6)
HheG2	26 ± 2 (50:50)	96 ± 0.9 (50:50)	< 0.01 (n.d. <sup>[b]</sup> )	17 ± 4.4 (76:24)	24 ± 2.1 (0.4:99.6)
Control	1.6 ± 0.5 (50:50)	1.6 ± 0.6 (50:50)	< 0.01 (n.d. <sup>[b]</sup> )	< 0.01 (n.d. <sup>[b]</sup> )	0.8 ± 0.1 (1:99)

[a] Original strains and accession numbers of all enzymes are listed in Table S1 in the supporting information. [b] not determined



**Scheme 2.** Possible regio- and stereoisomers in the azidolysis of vicinally di-substituted *trans*-epoxides 1–5. The site of attack ( $\alpha$ : less sterically hindered, shown in blue;  $\beta$ : sterically more hindered, shown in plum) defines the regioisomers obtained, while the enantioselectivity of the enzyme and the  $S_N2$ -type mechanism define the absolute configuration found in each set of regioisomers. Hence, a total of two regioisomers **a** and **b**, each with their respective (*R,S*)- and (*S,R*)-enantiomers, can be obtained.

(Table 1). HheA3, HheC and all tested E-type enzymes exhibited high regioselectivity for substrates 1 and 2, giving 2-azidohexan-3-ol (**6a**) and 2-azidoheptan-3-ol (**7a**) almost exclusively. In contrast, enzymes from the HDDH subfamily D as well as HheG and HheG2 formed both regioisomers (**6a** and **6b**, as well as **7a** and **7b**) in roughly equal amounts. The same was observed for chemical background azidolysis of 1 and 2 ("Control" in Table 1).

Compared to the conversion of 1, the terminal hydroxyl group present in 3 had a positive effect on HheG's regioselectivity. The enzyme produced 5-azidohexane-1,4-diol (**8a**) with high preference (Table 1). None of the active enzymes seemed to display high regioselectivity in the conversion of 4 as in all cases both azidoalcohol regioisomers **9a** and **9b** were formed. This might not be surprising considering that both substituents

of the epoxide ring are rather similar in size, differing only in one  $\text{CH}_2$  group.

In accordance with literature,<sup>[13,15]</sup> none of the tested enzymes exhibited a preference for formation of regioisomer **b**, except in the conversion of epoxide 5. Here, HheG and HheG2 gave azidoalcohol **10b** almost exclusively, whereas HheD3 and HheF formed also small amounts of regioisomer **10a**. Chemical azidolysis of epoxide 5 afforded **10b** almost exclusively as well. In this specific case, nucleophilic attack on the benzylic carbon is favoured due to the electronic resonance effect of the aromatic substituent.

Furthermore, the enantioselectivity of all active enzymes in the ring-opening of racemic epoxides 1 and 2 was analysed. For this, product enantiomeric excesses ( $ee_p$ ) and corresponding apparent  $E$ -values for each of the two possible product regioisomers were determined. As a result, most azidoalcohols were formed with low to moderate enantioselectivity (Table 2). Several HDDHs, however, displayed good enantioselectivity ( $E > 15$ ) in the formation of azidoalcohol regioisomers **6b** and **7b**.

Hence, nucleophilic attack on the unfavoured carbon atom occurred with higher enantioselectivity. Interestingly, most azidoalcohol products in the conversion of 1 and 2 were preferentially formed in 2*S*,3*R*-configuration. This indicates that epoxides 1 and 2 with *R,R*-configuration were preferentially attacked at the sterically less hindered carbon atom (C2), whereas regioisomers **6b** and **7b** were preferentially formed by nucleophilic attack of (*S,S*)-1 and (*S,S*)-2 at the sterically more hindered carbon atom (C3). In contrast, nucleophilic attack of azide at C2 in (*S,S*)-1 and (*S,S*)-2 yields azidoalcohols **6a** and **7a** in 2*R*,3*S*-configuration, as found for HheA3, HheE2, HheF and HheG2 with epoxide 1 and HheE4 and HheF with epoxide 2 (Table 2). A detailed analysis of the enzymes' regiopreferences in the azidolysis of *R,R*- and *S,S*-enantiomers of epoxides 1 and 2 is given in Table S3 in the supporting information. Interestingly, D-type HDDHs displayed a slightly higher preference for

**Table 2.** Conversions (C), enantiomeric excesses ( $ee_p$ ) and calculated apparent enantiomeric ratios ( $E^{app}$ ) of regioisomeric azidoalcohols **6a,b** and **7a,b** formed in the HDDH-catalysed azidolysis of epoxides 1 and 2. The absolute configuration of the preferentially formed enantiomer of each regioisomer is given in parentheses.

HDDH <sup>[a]</sup>	<b>6a</b> C [%]	$ee_p$ [%]	$E^{app}$	<b>6b</b> C [%]	$ee_p$ [%]	$E^{app}$	<b>7a</b> C [%]	$ee_p$ [%]	$E^{app}$	<b>7b</b> C [%]	$ee_p$ [%]	$E^{app}$
HheA3	48	47	4.2 ( <i>R,S</i> )	4.1	46	2.8 ( <i>S,R</i> )	93	0.7	1.0 ( <i>S,R</i> )	3.4	25.5	1.7 ( <i>S,R</i> )
HheB3	9.7	35	2.2 ( <i>S,R</i> )	3.6	66	5.0 ( <i>S,R</i> )	8.7	30	1.9 ( <i>S,R</i> )	4.3	77	7.7 ( <i>S,R</i> )
HheB5	52	25	2.1 ( <i>S,R</i> )	7.1	86	14 ( <i>S,R</i> )	85	24	1.6 ( <i>S,R</i> )	13	95	39 ( <i>S,R</i> )
HheB6	69	24	2.6 ( <i>S,R</i> )	7.6	89	18 ( <i>S,R</i> )	88	16	1.4 ( <i>S,R</i> )	11	93	28 ( <i>S,R</i> )
HheB7	73	24	2.9 ( <i>S,R</i> )	8.1	93	30 ( <i>S,R</i> )	89	17	1.4 ( <i>S,R</i> )	11	94	32 ( <i>S,R</i> )
HheC	43	34	2.6 ( <i>S,R</i> )	1.3	n.d. <sup>[b]</sup>	n.d. <sup>[b]</sup>	97	4.6	1.1 ( <i>S,R</i> )	2.3	90	19 ( <i>S,R</i> )
HheD	22	28	1.9 ( <i>S,R</i> )	22	86	17 ( <i>S,R</i> )	51	60	4.0 ( <i>S,R</i> )	43	87	14 ( <i>S,R</i> )
HheD2	32	22	1.7 ( <i>S,R</i> )	32	84	17 ( <i>S,R</i> )	45	57	3.7 ( <i>S,R</i> )	45	78	8.1 ( <i>S,R</i> )
HheD3	44	65	7.7 ( <i>S,R</i> )	44	43	3.4 ( <i>S,R</i> )	56	76	7.4 ( <i>S,R</i> )	43	80	9.0 ( <i>S,R</i> )
HheD5	64	46	6.5 ( <i>S,R</i> )	36	44	3.2 ( <i>S,R</i> )	50	13	1.3 ( <i>S,R</i> )	50	11	1.2 ( <i>S,R</i> )
HheE	98	4.9	1.1 ( <i>S,R</i> )	1.7	n.d. <sup>[b]</sup>	n.d. <sup>[b]</sup>	99	3.5	1.1 ( <i>S,R</i> )	0.8	n.d. <sup>[b]</sup>	n.d. <sup>[b]</sup>
HheE2	10	71	6.4 ( <i>R,S</i> )	1.1	n.d. <sup>[b]</sup>	n.d. <sup>[b]</sup>	83	11	1.2 ( <i>S,R</i> )	1.5	n.d. <sup>[b]</sup>	n.d. <sup>[b]</sup>
HheE3	14	4.5	1.1 ( <i>R,S</i> )	1.8	n.d. <sup>[b]</sup>	n.d. <sup>[b]</sup>	90	2.3	1.0 ( <i>S,R</i> )	1.4	n.d. <sup>[b]</sup>	n.d. <sup>[b]</sup>
HheE4	< 0.1	n.d. <sup>[b]</sup>	n.d. <sup>[b]</sup>	n.d. <sup>[b]</sup>	n.d. <sup>[b]</sup>	n.d. <sup>[b]</sup>	14	33	2.0 ( <i>R,S</i> )	0.5	n.d. <sup>[b]</sup>	n.d. <sup>[b]</sup>
HheE5	84	13	2.2 ( <i>S,R</i> )	1.8	n.d. <sup>[b]</sup>	n.d. <sup>[b]</sup>	99	3.5	1.1 ( <i>S,R</i> )	0.6	n.d. <sup>[b]</sup>	n.d. <sup>[b]</sup>
HheF	48	54	5.4 ( <i>R,S</i> )	8.0	32	2.0 ( <i>S,R</i> )	58	32	1.9 ( <i>R,S</i> )	12	19	1.5 ( <i>S,R</i> )
HheG	50	16	1.6 ( <i>S,R</i> )	50	15	1.5 ( <i>S,R</i> )	60	63	4.4 ( <i>S,R</i> )	40	89	17 ( <i>S,R</i> )
HheG2	13	54	3.6 ( <i>R,S</i> )	13	67	5.6 ( <i>S,R</i> )	48	7.4	1.2 ( <i>S,R</i> )	48	10	1.2 ( <i>S,R</i> )

[a] Original strains and accession numbers of all enzymes are listed in Table S1 in the supporting information. [b] not determined

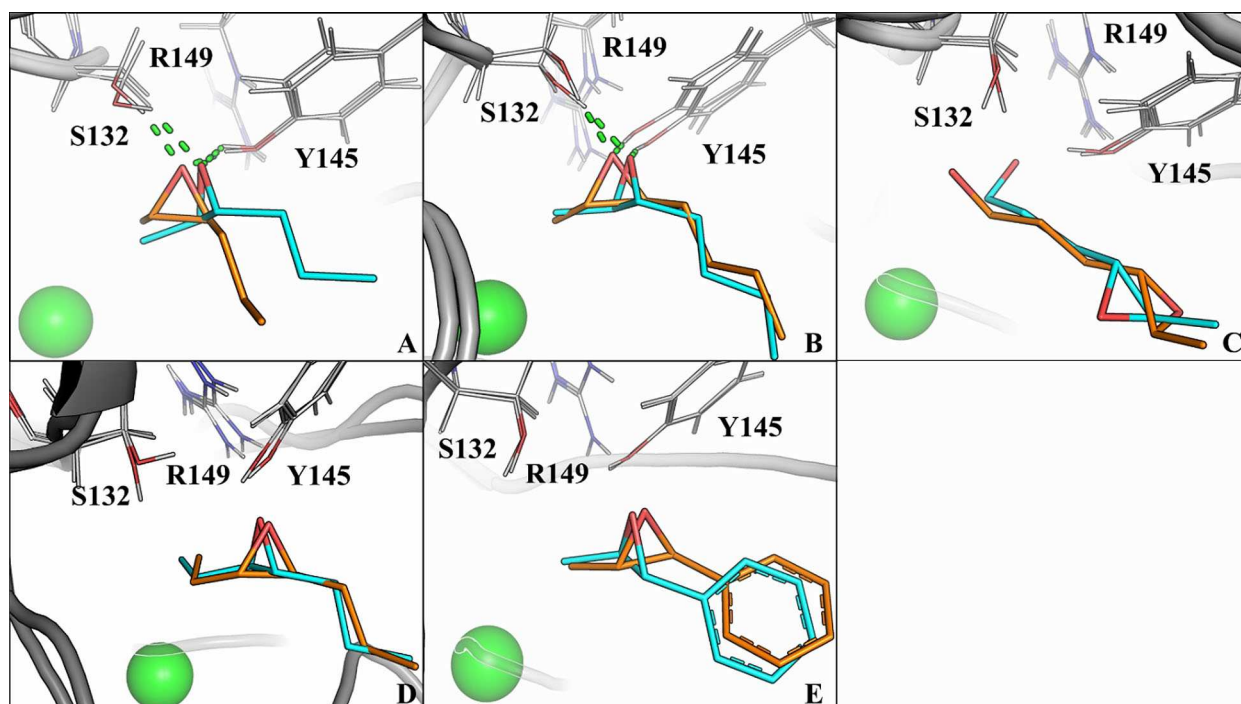


**Figure 1.** Docking results for HheC (PDB: 1ZMT) with substrates 1 (A), 2 (B), 3 (C), 4 (D) and 5 (E). Substrates with *R,R*-configuration are shown in light blue, while substrates with *S,S*-configuration are shown in orange. Hydrogen bonds between epoxide oxygen and catalytic residues S132 and Y145 are represented as green dotted lines. The water molecule present in the nucleophile binding pocket is shown as green sphere to indicate the position of the nucleophile.

nucleophilic attack of (*S,S*)-1 and (*S,S*)-2 at the sterically more hindered carbon atom, whereas most other HDDHs exhibited a clear preference for nucleophilic attack of the sterically less hindered carbon atom independent of the substrate's stereo-configuration. Additionally, the enantioselectivity of active HDDHs in the ring-opening of *rac*-5 was determined and results are given in Table S2 in the supporting information. No enantioselectivity was observed in the chemical epoxide ring opening of 1, 2 and 5 on preparative scale with azide as nucleophile (data not shown).

Among the tested halohydrin dehalogenases, HheG was the only enzyme able to convert all five epoxide substrates. This might be explained by the broad and open active site which is present in HheG's crystal structure.<sup>[19]</sup> In contrast, other HDDHs with solved crystal structure, namely HheA/A2, HheB/B2 and HheC<sup>[13,20,21]</sup> possess active sites that are more buried within the protein structure, with a rather narrow substrate channel leading to the active site. Hence, the broad active site cleft of HheG likely offers more space for the binding of bulky substrates such as the herein tested vicinally di-substituted epoxides. This is also supported by calculations of the active site volume of HheG, which was found to be 2.7 times larger than the calculated active site volume of HheC.<sup>[19]</sup> On the other hand, epoxide substrates with much bulkier substituents on both carbon atoms of the epoxide ring are likely not accepted by HheG as it was previously shown that *trans*-stilbene oxide was not converted by HheG or other tested HDDHs.<sup>[18]</sup>

HheC from *A. tumefaciens* was previously demonstrated to be *R*-selective, especially in the conversion of terminal aromatic

epoxides. This enantioselectivity is caused by non-productive binding of the respective (*S*)-epoxides in the active site of HheC.<sup>[15]</sup> Here, this HDDH seems significantly less stereoselective in the conversion of 1 and 2 as products **6a** and **7a** have been obtained with rather low ee (34% and 5%, respectively). On the other hand, HheC displayed very high regioselectivity yielding azidoalcohol regioisomers **6a** and **7a** almost exclusively. The regioselectivity of a HDDH during epoxide ring opening of vicinally di-substituted epoxides is determined by the exact positioning of epoxide substrate and nucleophile in the active site of the enzyme. This relative positioning of epoxide ring and nucleophile to each other will dictate which of the two carbon atoms of the epoxide ring can be attacked by the nucleophile. To investigate this in more detail for HheC, molecular docking of both enantiomers of epoxides 1–5 into the enzyme's active site was performed. This revealed that both substrate enantiomers of 1 and 2 bind in similar productive orientations with the methyl-substituted carbon atom in closer proximity to the nucleophile binding pocket (Figure 1A and B). This is in line with our experimental data that both epoxide enantiomers can be converted by HheC, but the methyl-substituted carbon atom is always attacked preferentially, resulting in the observed high regio- but low enantioselectivity of this enzyme. In contrast, docking of (*R,R*)- and (*S,S*)-4 yielded possible binding modes with the epoxide oxygen being too far away from the serine of the catalytic triad to facilitate catalysis (Figure 1D).

Similarly, for both enantiomers of epoxide 5 no binding mode with the epoxide oxygen in hydrogen bonding distance to the catalytic triad serine and tyrosine of HheC was observed



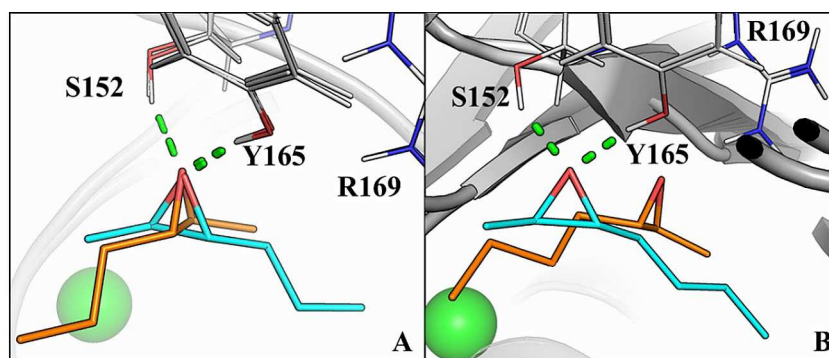


**Figure 2.** Docking results for HheG (PDB: 5O30) with substrates 1 (A) and 2 (B). Substrates with *R,R*-configuration are shown in light blue, while substrates with *S,S*-configuration are shown in orange. Hydrogen bonds between epoxide oxygen and catalytic residues S152 and Y165 are represented as green dotted lines. The water molecule present in the nucleophile binding pocket is shown as green sphere to indicate the position of the nucleophile.

(Figure 1E). This is again in agreement with our experimental data obtained for HheC, which did not convert epoxides 4 and 5. Docking of epoxide 3 revealed non-productive binding modes for both substrate enantiomers with the terminal hydroxyl group pointing towards the catalytic amino acid residues (Figure 1C). This flipped binding mode of 3 found for HheC might also occur in other HDDHs and could thus explain the lack of activity of most HDDHs toward this epoxide. Since possible unproductive binding modes could be obtained for 3, 4 and 5, all three epoxides might act as inhibitors of HheC.

For comparison, similar dockings of epoxides 1–5 were also performed with HheG. Here, possible productive binding modes of both enantiomers of 1 and 2 were obtained with the epoxide oxygen in hydrogen bonding distance to the catalytic serine and tyrosine (Figure 2). In contrast to HheC, however, both substrate enantiomers display different orientations with the longer alkyl side chain pointing in opposite directions. This is only possible due to the much larger active site cavity of HheG compared to HheC. With the other three substrates (3–5) and HheG, the docking results are less informative as not all substrate enantiomers yielded possible productive binding modes (Supporting Information, S4). This is not surprising considering that no substrate-bound structure of HheG is available yet. Hence, the resulting substrate binding poses found for HheG may not reflect the real binding modes. In case of HheC, molecular dockings were performed using an epoxide-bound enzyme structure (PDB: 1ZMT).<sup>[15]</sup> Therefore, the obtained docking results will be more reliable. As no crystal structure of a member of HDDH subfamily E has been determined so far, no structural insights into the observed high regioselectivity could be gained for these enzymes.

Selected regioselective HDDH-catalysed reactions were also performed on preparative scale to demonstrate the synthetic potential of this class of enzymes. For this, epoxide substrates 1 and 2 were each converted with a regioselective HDDH (HheE for substrate 1 and HheE5 for substrate 2) by means of whole-cell biocatalysis. Using each 200 mg (50 mM) of epoxide per reaction, 142 mg of regioisomer **6a** and 151 mg of regioisomer **7a** (50% and 48% isolated yield, respectively) were obtained in pure form.

## Conclusions

A set of 22 halohydrin dehalogenases, representing all currently known phylogenetic subtypes, was studied in the azidolysis of five vicinally di-substituted epoxides. The majority of these enzymes displayed significant activity towards simple aliphatic epoxides that carried a methyl group at one of the carbon atoms of the epoxide ring. Several HDDHs were even found to be highly regioselective, facilitating the synthesis of regioisomerically pure azidoalcohols on preparative scale. HheG from *Ilumatobacter coccineus* converted also sterically more demanding non-terminal epoxides with good to high activity. Overall, the observed regio- and stereoselectivity of active enzymes towards the tested vicinally di-substituted epoxides was found to be enzyme- and substrate-dependent. Docking studies based on an epoxide-bound structure of HheC revealed first structural insights into the observed substrate and regio-selectivity of this enzyme.

With this, we could demonstrate that the substrate scope of HDDHs is not limited to terminal epoxides. Instead, they can be applied in the conversion of non-terminal epoxide substrates, thus, expanding the range of accessible  $\beta$ -substituted alcohols. This further broadens the biocatalytic applicability of HDDHs, in particular of HheG, substantially. Further improvement of the enzymes' enantioselectivities by protein engineering will enable the synthesis of optically pure products in the future.

## Experimental Section

### Chemicals

*Trans*-2-hexene was purchased from Acros Organics (Geel, Belgium), *trans*-2-heptene was purchased from abcr GmbH (Karlsruhe, Germany). *Trans*- $\beta$ -methylstyrene and *trans*-3-heptene were purchased from TCI Deutschland GmbH (Eschborn, Germany). *Trans*-2-hexen-1-ol was purchased from J&K Scientific (Lommel, Belgium). (1*S*,2*S*)-(-)-1-phenylpropylene oxide and (1*R*,2*R*)-(+)-1-phenylpropylene oxide were purchased from Sigma-Aldrich (Darmstadt, Germany).

Racemic epoxides *trans*-2,3-epoxyhexane (**1**) and *trans*-2,3-epoxyheptane (**2**) were synthesised according to Sharma et al. using a slightly modified protocol.<sup>[22]</sup> Epoxidations were carried out in CH<sub>2</sub>Cl<sub>2</sub> (40 mL g<sup>-1</sup> of alkene). *m*-Chloroperbenzoic acid (1.5 eq.) was added in small portions over 15 min at room temperature (RT). After 1 h at RT, the mixture was stirred on ice for 5 min and the white slurry was filtered. 5% w/v aq. Na<sub>2</sub>SO<sub>3</sub> (40 mL g<sup>-1</sup> alkene) was added and stirred at RT for 15 min, then the phases were separated. The aqueous layer was extracted two times with CH<sub>2</sub>Cl<sub>2</sub>. The combined organic layers were washed with sat. aq. NaHCO<sub>3</sub> (1×) and brine (1×), dried over MgSO<sub>4</sub> and filtered before solvent removal by evaporation. The epoxides were purified by column chromatography using a mixture of cyclohexane/ethyl acetate, 95:5.

Racemic *trans*-4,5-epoxyhexan-1-ol (**3**), *trans*-3,4-epoxyheptane (**4**) and *trans*-β-methylstyrene oxide (**5**) were synthesised by mixing the respective alkene to a final concentration of 200 mM in water with 30% acetonitrile and 10% of acetone. 3 eq. of oxone® were added portion-wise over 4 hours. The pH was kept at 8 by adding NaHCO<sub>3</sub> to the solution.<sup>[23]</sup> The reactions were followed by TLC. When all substrate was converted, the reaction mixture was extracted three times with *tert*-butylmethyl ether (TBME). The combined organic layers were washed with brine (1×), dried over Na<sub>2</sub>SO<sub>4</sub> and filtered before solvent removal by evaporation. The epoxides were purified by column chromatography with cyclohexane/isopropanol (95:5) for **3**, cyclohexane/ethyl acetate (95:5) for **4** and cyclohexane/ethyl acetate (90:10) for **5**. Formation and purity of the epoxides was confirmed by NMR and resulting NMR data were consistent with literature data.<sup>[24–26]</sup>

### Bacterial Strains and Plasmids

The strains *Escherichia coli* BL21(DE3) (Life Technologies, Darmstadt, Germany), *E. coli* C43(DE3) (Lucigen Corporation, Middleton, WI, USA) and *E. coli* Top10 (Life Technologies) were used as hosts for heterologous protein production. All HDDH genes except *hheA2*, *hheB2* and *hheC* were expressed from pET28a(+)-based vectors, utilizing a T7 promoter and resulting in a N-terminal hexahistidin (His6) tag fusion.<sup>[17]</sup> Instead, vectors pBAD-*hheA2*, pBAD-*hheB2* and pBAD-*hheC*, utilizing an arabinose-inducible promoter, were used for the expression of the *HheA2*, *HheB2* and *HheC* genes, respectively, as described previously.<sup>[12,27]</sup>

### Expression and Purification of HDDHs

All HDDH enzymes except *HheE4* and *HheG2* were produced and purified as reported previously.<sup>[12,18]</sup> Enzymes *HheE4* and *HheG2* were produced in *E. coli* BL21(DE3). Respective overnight cultures were used to inoculate (10% v/v) 500 mL TB medium (4 mL<sup>-1</sup> glycerol, 12 g L<sup>-1</sup> peptone, 24 g L<sup>-1</sup> yeast extract, 0.17 M KH<sub>2</sub>PO<sub>4</sub>, 0.74 M K<sub>2</sub>HPO<sub>4</sub>) supplemented with 50 mg L<sup>-1</sup> kanamycin and 0.2 mM IPTG. Expression cultures were grown at 22 °C for 24 h. Cells were harvested by centrifugation (4,400 g, 20 min at 4 °C) and cell pellets were stored at –20 °C until further use. Both enzymes were purified via affinity chromatography according to a previously published protocol.<sup>[18]</sup> A list of all HDDHs used in this work with their respective source organisms and accession numbers is given in Table S2 in the supporting information.

### General Biotransformation Experiment

Small-scale biotransformations (1 mL) were performed in 50 mM potassium phosphate buffer at pH 7.5 containing 150 µg mL<sup>-1</sup> HDDH enzyme, 5 mM substrate (**1**–**5**) and 20 mM sodium azide

(NaN<sub>3</sub>) at 25 °C. After 15 h (substrates **1**–**4**) or 4 h (substrate **5**) of reaction, an aliquot of 400 µL was taken and extracted with the same volume of TBME containing 0.1% v/v dodecane as internal standard. The resulting organic phase was dried over anhydrous MgSO<sub>4</sub> prior to injection on GC or GC-MS. All biotransformations were carried out in duplicate. Chemical background azidolysis was monitored in reactions using the same reaction conditions but omitting HDDH enzyme.

### Determination of Enantiomeric Excesses

In order to distinguish *trans*-(2*S*,3*S*)-epoxyhexane and *trans*-(2*R*,3*R*)-epoxyhexane as well as *trans*-(2*S*,3*S*)-epoxyheptane and *trans*-(2*R*,3*R*)-epoxyheptane on chiral GC, *trans*-(2*S*,3*S*)-epoxyhexane (*S,S*-**1**) and *trans*-(2*S*,3*S*)-epoxyheptane (*S,S*-**2**) were selectively synthesised according to a published protocol using *E. coli* whole cells harbouring the styrene monooxygenase (StyAB) from *Rhodococcus* sp. ST-10.<sup>[28,29]</sup> Assignment of all azidoalcohol enantiomers on chiral GC was achieved by further conversion of the obtained (*S,S*)-**1** and (*S,S*)-**2** using each a regioselective and a non-regioselective HDDH. Using a regioselective HDDH (*HheE5* for **2** and *HheE* for **1**), only (2*R*,3*S*)-**6a** and (2*R*,3*S*)-**7a** are produced, while using non-regioselective enzymes (*HheD5* for **2** and *HheG* for **1**), (2*R*,3*S*)-**6a**, (2*S*,3*R*)-**6b**, (2*R*,3*S*)-**7a** and (2*S*,3*R*)-**7b** are obtained. Reactions were performed in 50 mM potassium phosphate buffer at pH 7.5 using 5 mM (*S,S*)-**1** or (*S,S*)-**2**, 150 µg mL<sup>-1</sup> HDDH and 20 mM sodium azide at 25 °C. After 15 h, an aliquot of 400 µL was taken and extracted with the same volume of TBME containing 0.1% v/v dodecane as internal standard. The resulting organic phase was dried over anhydrous MgSO<sub>4</sub> before injection on chiral GC. GC-MS analysis of the same material was performed to assign the different regioisomers of **6** and **7**.

The assignment of enantiomers of azidoalcohols **10a** and **10b** on chiral GC was performed in a similar way starting from commercially available enantiopure epoxides (*S,S*)-**5** and (*R,R*)-**5**. Due to the S<sub>N</sub>2-type mechanism and the observed regioselectivity of the chemical azidolysis of **5**, chemical conversion of (*S,S*)-**5** lead to an excess of (1*R*,2*S*)-1-azido-1-phenylpropan-2-ol (**10b**) next to a small amount of (1*S*,2*R*)-2-azido-1-phenylpropan-1-ol (**10a**). In contrast, ring-opening of the opposite enantiomer (*R,R*)-**5** generated (1*S*,2*R*)-1-azido-1-phenylpropan-2-ol (**10b**) in excess and a small amount of (1*R*,2*S*)-2-azido-1-phenylpropan-1-ol (**10a**).

### Preparative Scale Biotransformation

Preparative-scale conversions of **1** and **2** were performed using whole cells of *E. coli* harbouring either *HheE*, or *HheE5*. All biotransformations were performed in 40 mL of 50 mM potassium phosphate buffer at pH 7.5 containing a cell density of OD<sub>600</sub> = 40 (equivalent to 60 g wet cells per litre reaction), 50 mM of either **1** or **2** and 100 mM sodium azide (NaN<sub>3</sub>). After 24 h at 25 °C, the reaction mixture was extracted with 40 mL TBME and filtered through Celite®. The extracted organic layer was washed with brine (1×) and MilliQ water (1×), dried over Na<sub>2</sub>SO<sub>4</sub> and filtered before solvent evaporation. 142 mg (50% yield) of **6a** and 151 mg (48% yield) of **6b** could be recovered after column chromatography using cyclohexane/diethyl ether, 90:10.

### Chemical Synthesis of Authentic Azidoalcohol Standards

1 mmol of either *trans*-2,3-epoxyhexane (100 mg) or *trans*-2,3-epoxyheptane (114 mg) were mixed with 202 mg of NaN<sub>3</sub> (3.1 eq.) and 166 mg of NH<sub>4</sub>Cl (3.1 eq.) in 3.5 mL methanol and refluxed at 65 °C until no more substrate was visible on TLC (5–6 h). The

reaction mixture was then diluted with diethyl ether, washed with brine, the water phase was then extracted twice with diethyl ether. The organic layers were combined and dried over  $\text{Na}_2\text{SO}_4$ . The crude extracts were purified by column chromatography (cyclohexane/diethyl ether, 90:10) yielding 52% azidoheptanol (**6**) and 48% azidoheptanol (**7**).<sup>[30]</sup>

Following a similar protocol, azidoalcohols **8**, **9** and **10** were synthesised by dissolving the corresponding epoxides **3–5** in MeOH with 5%  $\text{H}_2\text{O}$  to a final concentration of 200 mM,  $\text{NaN}_3$  (3.1 eq.) and  $\text{NH}_4\text{Cl}$  (3.1 eq.) were added and the reaction was stirred over night at 65 °C under reflux. Methanol was evaporated, the crude extract was dissolved in TBME and washed with the same volume of brine (1×). The water phase was extracted three times with TBME. The combined organic layers were dried over  $\text{Na}_2\text{SO}_4$  and filtered before solvent removal by evaporation. Diastereomeric mixtures of **8a/b**, **9a/b** and **10a/b** were purified by column chromatography using chloroform/acetone, 95:5; cyclohexane/ethyl acetate, 95:5, and heptane/ethyl acetate, 70:30, respectively.

**Diastereomeric mixture of 2-azidoheptan-3-ol (6a) and 3-azidoheptan-2-ol (6b):** pale oil,  $^1\text{H}$  NMR (600 MHz,  $\text{CDCl}_3$ )  $\delta$  = 3.90–3.81 (m, 1H, **6b**), 3.65–3.58 (m, 1H, **6a**), 3.52 (dq,  $J$  = 6.7, 3.9, 1H, **6a**), 3.42–3.35 (m, 1H, **6b**), 1.61–1.29 (m, 14H, **6a** and **6b**), 1.25 (d,  $J$  = 6.7, 3H, **6a**), 1.19 (d,  $J$  = 6.4, 3H, **6b**), 0.96 (t,  $J$  = 7.2, 3H, **6b**), 0.94 (t,  $J$  = 7.3, 3H, **6a**).  $^{13}\text{C}$  NMR (151 MHz,  $\text{CDCl}_3$ )  $\delta$  = 73.55 (**6a**), 69.99 (**6b**), 67.92 (**6b**), 61.77 (**6a**), 34.57 (**6a**), 32.07 (**6b**), 19.65 (**6b**), 18.96 (**6a**), 18.13 (**6b**), 13.91 (**6a**), 13.80 (**6b**), 13.11 (**6a**). ESI-HRMS:  $[\text{M} + \text{Na}^+] = 166.09524$  m/z (calculated  $[\text{M} + \text{Na}^+] = 166.09508$  m/z).

**Diastereomeric mixture of 2-azidoheptan-3,6-diol (8a) and 3-azidoheptan-2,6-diol (8b):** pale oil,  $^1\text{H}$  NMR (600 MHz,  $\text{CDCl}_3$ )  $\delta$  = 3.92–3.85 (m, 2H, **8b**), 3.82–3.60 (m, **8a** 3H, **8b** 1H), 3.50–3.44 (m, 1H, **8a**), 3.42–3.40 (m,  $J$  = 4.98, 1H, **8b**), 2.86 (s, 1H, **8a**), 2.63 (s, 1H, **8b**), 2.34 (s, 1H, **8a**), 2.17 (s, 1H, **8b**), 1.65–1.34 (m, 8H, **8a** and **8b**), 0.97 (t,  $J$  = 7.0, 3H, **8a**), 0.96 (t,  $J$  = 6.9, 3H, **8b**).  $^{13}\text{C}$  NMR (151 MHz,  $\text{CDCl}_3$ )  $\delta$  = 73.80 (**8a**), 72.39 (**8b**), 67.04 (**8b**), 64.64 (**8a**), 63.33 (**8a**), 62.60 (**8b**), 36.00 (**8b**), 32.83 (**8a**), 19.74 (**8a**), 19.01 (**8b**), 14.13 (**8b**), 14.03 (**8a**). ESI-HRMS:  $[\text{M} + \text{Na}^+] = 182.09010$  m/z (calculated  $[\text{M} + \text{Na}^+] = 182.0905$  m/z).

**Diastereomeric mixture of 3-azidoheptan-4-ol (9a) and 4-azidoheptan-3-ol (9b):** pale oil,  $^1\text{H}$  NMR (600 MHz,  $\text{CDCl}_3$ )  $\delta$  = 3.72–3.64 (m, 1H, **9a**), 3.62–3.55 (m, 1H, **9b**), 3.42–3.32 (m, 1H, **9b**), 3.31–3.23 (m, 1H, **9a**), 1.73–1.31 (m, 14H, **9a** and **9b**), 1.04 (t,  $J$  = 7.4 Hz, 3H, **9a**), 1.00 (t,  $J$  = 7.4 Hz, 3H, **9b**), 0.96 (t,  $J$  = 7.1 Hz, 3H, **9b**), 0.95 (t,  $J$  = 7.2 Hz, 3H, **9a**).  $^{13}\text{C}$  NMR (151 MHz,  $\text{CDCl}_3$ )  $\delta$  = 75.64 (**9b**), 73.64 (**9a**), 69.46 (**9a**), 67.26 (**9b**), 34.70 (**9a**), 31.74 (**9b**), 25.58 (**9b**), 22.90 (**9a**), 19.93 (**9b**), 19.20 (**9a**), 14.20 (**9a**), 14.10 (**9b**), 11.24 (**9a**), 10.43 (**9b**). ESI-HRMS:  $[\text{M} + \text{Na}^+] = 180.11081$  m/z (calculated  $[\text{M} + \text{Na}^+] = 180.1112$  m/z).

Obtained NMR data for **7a/b**<sup>[30]</sup> and **10a/b**<sup>[31,32]</sup> were consistent with literature data.

## Analytical Methods

Achiral GC analysis was performed on a GC-2010 plus gas chromatograph (Shimadzu, Duisburg, Germany) equipped with an Optima 5 ms column (Macherey-Nagel, Düren, Germany) and FID detection using hydrogen as carrier gas. Chiral GC analysis was performed on a GC-2010 plus gas chromatograph (Shimadzu) equipped with two different chiral columns and FID detection using hydrogen as carrier gas. A Lipodex E column (Macherey-Nagel) was used for the separation of azidoalcohol products **6–10**, whereas a HYDRODEX  $\gamma$ -DiMOM column (Macherey-Nagel) was used for the separation of epoxide substrates **1–5**. Temperature programs and

retention times are listed in Table S23 in the supporting information.

Conversions of epoxides into the corresponding azidoalcohols were determined by achiral GC based on relative peak areas. Ratios of regioisomers **6a/b**, **8a/b** and **9a/b** were calculated based on peak areas derived from chiral GC, whereas ratios of regioisomers **7a/b**, **10a/b**, were calculated based on peak areas derived from achiral GC. Enantiomeric excesses (ee) of azidoalcohol products **6**, **7** and **10** were calculated according to Chen et al. based on chiral GC data.<sup>[33]</sup> Apparent enantiomeric ratios ( $E^{app}$ ) of HHDHs for the formation of regioisomeric products **6a** and **6b**, **7a** and **7b** as well as **10a** and **10b** were calculated according to Chen et al. based on conversion (C) and product enantiomeric excess (ee).<sup>[33]</sup>

GC-MS analysis of azidoalcohol products was performed on a Shimadzu GCMS-QP2010SE equipped with a ZB-5MS GUARDIAN column (Phenomenex) and helium as carrier gas.

NMR spectra were recorded on a Bruker Avance 600 MHz spectrometer equipped with an inverse  $^1\text{H}/^{13}\text{C}/^{15}\text{N}/^{31}\text{P}$  quadruple resonance cryoprobe head and z field gradients. The sample was dissolved in deuterated chloroform ( $\text{CDCl}_3$ ) and 1D proton, DEPT, COSY double quantum filter, and HSQC experiments were performed at 25 °C. The regioisomers of chemically synthesised azidoalcohols **6**, **8** and **9** were identified by NMR spectroscopy employing COSY and HSQC techniques and further compared to the assignment of regioisomers by GC and GC-MS.

## Docking Studies

Molecular docking of MM2-force field energy minimized (*S,S*- and (*R,R*)-**1** to **5** into the active site of a monomeric representation of HheC (PDB-ID: 1ZMT) and HheG (PDB-ID: 5O30) was performed using the AutoDockVina program environment of YASARA Structure.<sup>[34,35]</sup> All ten substrate structures were docked into a simulation cell (X size = 25 Å, Y size = 25 Å, Z size = 25 Å; angles:  $\alpha = 90^\circ$ ,  $\beta = 90^\circ$ ,  $\gamma = 90^\circ$ ) around the four residues K91, L155, E197 and E216 for HheC and the corresponding residues D111, I175, E214 and E233 in HheG. For each substrate, 999 docking runs were performed with atoms and bonds of the corresponding substrates set as rigid. The only exception is substrate **3** with HheG where a flexible ligand was necessary to obtain one cluster with productive binding. Docking of each substrate resulted in one or more clusters of similar binding modes which were energy minimized using the YASARA2-force field after inserting the water molecule of the nucleophile binding pocket as fixed element. This water molecule is present in the respective crystal structures and represents the position of the nucleophile in the binding pocket. Figures of the structures with docked ligands were generated with PyMOL Molecular Graphics System version 2.2.3 (Schrödinger, LLC, New York, NY, USA).

## Acknowledgements

We thank Dr. Melinda Fekete from Enzymicals for helpful advice regarding chemical syntheses. This work has received funding from the European Union's Horizon 2020 MSCA ITN-EID program under grant agreement No 634200 (BIOCASCADES) and the Horizon 2020 research and innovation programme under grant agreement No 635595 (CARBAZYMES). This communication reflects only the beneficiary's view and the European Commission is not responsible for any use that may be made of the information it contains.

## Conflict of Interest

This work has been performed in collaboration with the company Enzymicals AG within the Horizon 2020 projects BIOCASCADES and CARBAZYMES. Enzymicals markets the respective halohydrin dehalogenases. Dr. Rainer Wardenga and Dr. Philipp Süss from Enzymicals are co-authors of this manuscript.

**Keywords:** Biocatalysis · Enzymes · Epoxide ring opening · Halohydrin dehalogenase · Regioselectivity

- [1] C. E. Castro, E. W. Bartnicki, *Biochemistry* **1968**, *7*, 3213–3218.
- [2] Z.-Y. You, Z.-Q. Liu, Y.-G. Zheng, *Appl. Microbiol. Biotechnol.* **2013**, *97*, 9–21.
- [3] A. Schallmeyer, M. Schallmeyer, *Appl. Microbiol. Biotechnol.* **2016**, *100*, 7827–7839.
- [4] G. Hasnaoui-Dijoux, M. Majerić Elenkov, J. H. Lutje Spelberg, B. Hauer, D. B. Janssen, *ChemBioChem* **2008**, *9*, 1048–1051.
- [5] E. J. de Vries, D. B. Janssen, *Curr. Opin. Biotechnol.* **2003**, *14*, 414–420.
- [6] N.-W. Wan, Z.-Q. Liu, K. Huang, Z.-Y. Shen, F. Xue, Y.-G. Zheng, Y.-C. Shen, *RSC Adv.* **2014**, *4*, 64027–64031.
- [7] H. M. S. Assis, A. T. Bull, D. J. Hardman, *Enzyme Microb. Technol.* **1998**, *22*, 545–551.
- [8] T. Nakamura, T. Nagasawa, F. Yu, I. Watanabe, H. Yamada, *Tetrahedron* **1994**, *50*, 11821–11826.
- [9] M. M. Elenkov, L. Tang, A. Meetsma, B. Hauer, D. B. Janssen, *Org. Lett.* **2008**, *10*, 2417–2420.
- [10] J. H. Lutje Spelberg, L. Tang, M. van Gelder, R. M. Kellogg, D. B. Janssen, *Tetrahedron: Asymmetry* **2002**, *13*, 1083–1089.
- [11] C. Molinaro, A.-A. Guibault, B. Kosjek, *Org. Lett.* **2010**, *12*, 3772–3775.
- [12] J. E. T. van Hylckama Vlieg, L. Tang, J. H. Lutje Spelberg, T. Smilda, G. J. Poelarends, T. Bosma, A. E. J. van Merode, M. W. Fraaije, D. B. Janssen, *J. Bacteriol.* **2001**, *183*, 5058–5066.
- [13] R. M. de Jong, J. J. W. Tiesinga, H. J. Rozeboom, K. H. Kalk, L. Tang, D. B. Janssen, B. W. Dijkstra, *EMBO J.* **2003**, *22*, 4933–4944.
- [14] R. M. de Jong, B. W. Dijkstra, *Curr. Opin. Struct. Biol.* **2003**, *13*, 722–730.
- [15] R. M. de Jong, J. J. W. Tiesinga, A. Villa, L. Tang, D. B. Janssen, B. W. Dijkstra, *J. Am. Chem. Soc.* **2005**, *127*, 13338–13343.
- [16] M. M. Elenkov, B. Hauer, D. B. Janssen, *Adv. Synth. Catal.* **2006**, *348*, 579–585.
- [17] M. Schallmeyer, J. Koopmeiners, E. Wells, R. Wardenga, A. Schallmeyer, *Appl. Environ. Microbiol.* **2014**, *80*, 7303–7315.
- [18] J. Koopmeiners, B. Halmschlag, M. Schallmeyer, A. Schallmeyer, *Appl. Microbiol. Biotechnol.* **2016**, *100*, 7517–7527.
- [19] J. Koopmeiners, C. Diederich, J. Solarczek, H. Voß, J. Mayer, W. Blankenfeldt, A. Schallmeyer, *ACS Catal.* **2017**, *7*, 6877–6886.
- [20] R. M. de Jong, K. H. Kalk, L. Tang, D. B. Janssen, B. W. Dijkstra, *J. Bacteriol.* **2006**, *188*, 4051–4056.
- [21] F. Watanabe, F. Yu, A. Ohtaki, Y. Yamanaka, K. Noguchi, M. Yohda, M. Odaka, *Proteins Struct. Funct. Bioinf.* **2015**, *83*, 2230–2239.
- [22] R. Sharma, P. G. Bulger, M. McNevin, P. G. Dormer, R. G. Ball, E. Streckfuss, J. F. Cuff, J. Yin, C. Chen, *Org. Lett.* **2009**, *11*, 3194–3197.
- [23] S. E. Denmark, Z. Wu, C. M. Crudden, H. Matsushashi, *J. Org. Chem.* **1997**, *62*, 8288–8289.
- [24] W. Kroutil, M. Mischitz, K. Faber, *J. Chem. Soc. Perkin Trans. 1* **1997**, *0*, 3629–3636.
- [25] E. G. Ankudey, H. F. Olivo, T. L. Peebles, *Green Chem.* **2006**, *8*, 923–926.
- [26] J. Lindborg, A. Tanskanen, L. T. Kanerva, *Biocatal. Biotransform.* **2009**, *27*, 204–210.
- [27] R. M. Haak, C. Tarabiono, D. B. Janssen, A. J. Minnaard, J. G. de Vries, B. L. Feringa, *Org. Biomol. Chem.* **2007**, *5*, 318–323.
- [28] H. Toda, R. Imae, N. Itoh, *Adv. Synth. Catal.* **2014**, *356*, 3443–3450.
- [29] H. Toda, R. Imae, N. Itoh, *Tetrahedron: Asymmetry* **2012**, *23*, 1542–1549.
- [30] G. Righi, S. Pietrantonio, C. Bonini, *Tetrahedron* **2001**, *57*, 10039–10046.
- [31] B. Yang, Z. Lu, *ACS Catal.* **2017**, *7*, 8362–8365.
- [32] I. A. Sayyed, A. Sudalai, *Tetrahedron: Asymmetry* **2004**, *15*, 3111–3116.
- [33] C. S. Chen, Y. Fujimoto, G. Girdaukas, C. J. Sih, *J. Am. Chem. Soc.* **1982**, *104*, 7294–7299.
- [34] G. M. Morris, D. S. Goodsell, R. S. Halliday, R. Huey, W. E. Hart, R. K. Belew, A. J. Olson, *J. Comput. Chem.* **1998**, *19*, 1639–1662.
- [35] O. Trott, A. J. Olson, *J. Comput. Chem.* **2010**, *31*, 455–461.

Manuscript received: January 17, 2019

Revised manuscript received: February 18, 2019

Version of record online: March 15, 2019